Application note

Providing automation platform for fill-finish quantification and qualitative assessment with model transferability

The Thermo Scientific™ DXR3 SmartRaman™+ Spectrometer

Authors

Nimesh Khadka[1], Ph.D.
Alec Fisher[2]
Robert Heintz[2], Ph.D.

[1]Analytical Instrument Group, Thermo Fisher Scientific, Tewksbury, Massachusetts USA
[2]Analytical Instrument Group, Thermo Fisher Scientific, Madison, Wisconsin USA

Industry/application

Biopharma / pharma

Products used

Thermo Scientific™ DXR3 SmartRaman™+ Spectrometer

Goals

1. Demonstrate the capability of DXR3 SmartRaman+ spectrometer for drug product identification and quantification
2. Demonstrate a data driven strategy to optimize the sampling position
3. Demonstrate the performance of direct model transferability across instruments
4. Provide evidence of transfer function-based model transferability across instruments to improve performance

Key words

Raman spectroscopy, drug products, active pharmaceutical ingredients (API), excipients, fill-finished products, model transferability

Key benefits

Rapid and reliable multi-attribute measurements, including identification and quantification of fill-finished products, with cost and time benefits.

Introduction

The biopharmaceutical market is growing rapidly, with many types of drug products already available in the market for a wide variety of treatments. These products include proteins such as monoclonal antibodies, peptides such as GLP-1, nucleic acids such as mRNA vaccines, conjugated or modified biomolecules such as antibody–drug conjugates, therapeutic cells such as CAR-T, and viruses such as AAV and Lentivirus.[1]

Manufacturing of biopharmaceuticals is highly regulated. Strict cGMP protocols ensure batch-to-batch reproducibility, safety, and efficacy. Recently, manufacturing and operational costs have risen worldwide. Quality control (QC) is a major cost driver. QC remains “unnegotiable” and still depends on many labor-intensive assays to monitor product quality attributes (PQAs) for release and stability. A better approach is to use simpler, faster, and automation-friendly analytical tools. These tools should monitor PQAs across the product lifecycle while maintaining high quality.[2]

Raman spectroscopy meets these needs. It is simple, nondestructive, and can read directly through various containers with little or no sample preparation. Raman analysis measures inelastic photon scattering; this signal is highly specific to target analytes. It reveals compositional, structural, and conformational information about drug products. Combined with multivariate data analysis, a single Raman spectrum can quantify multiple analytes and quality attributes in complex formulations. This enables streamlined, multi-attribute QC that supports diverse products, controls costs, and maintains quality. It reduces operational cost and time. It also enables larger QC sampling without extra cost or time, further improving quality assurance.

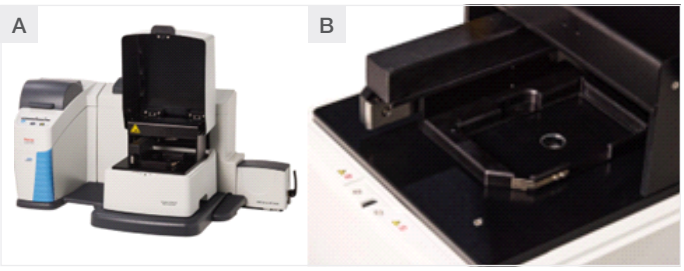

Figure 1. (a) DXR3 SmartRaman+ spectrometer with the ASA accessory installed. (b) ASA accessory with no sample holder.

This study demonstrates the capabilities of the Thermo Scientific™ DXR3 SmartRaman™+ spectrometer for quantitative and qualitative assessment of simulated drug products. The study also evaluates direct model transferability across several instruments, using different samples and laser sources, and outlines strategies to improve transferability. For this study, non-destructive measurements were obtained through glass containers. Overall, the newly introduced DXR3 SmartRaman+ spectrometer, with OPC-UA connectivity and an integrated autosampler (ASA), will be shown to provide a complete platform for fill-finish identification and quantification.

Experimental details

Sample preparations

Model transferability studies across DXR3 SmartRaman+ instruments were performed using low and high fluorescence samples in glass containers. For the low fluorescence samples, a 532 nm laser was used. Acetaminophen solutions from 0 to 10 mg/mL were prepared as 4 mL fills in 5 mL glass vials. Raman data were acquired on six different instruments. All measurements were taken through the sample vials.

A second set of transferability studies used a 785 nm laser for high fluorescence drug product samples. To mimic a fill-finish protein drug product, mixtures of bovine serum albumin (BSA), sucrose (a commonly used stabilizer), and methionine (a commonly used antioxidant) at varying concentrations were prepared in tris buffer at pH 8.0.[3,4] All samples were filled to 4 mL volume in 5 mL borosilicate glass vials. Training and validation concentrations were determined by a design of experiment (DoE) using a Uniform Design (UD) algorithm[5] (Figure 2).

Factors (Calibration)	Lower control limits (mg/mL)	Upper control limits (mg/mL)
BSA	0	30
Sucrose	0	50
Methionine	0	10

Factors (Validation)	Lower control limits (mg/mL)	Upper control limits (mg/mL)
BSA	1	28
Sucrose	0.5	45
Methionine	0.5	9.5

Sample	BSA (mg/mL)	Sucrose (mg/mL)	Methionine (mg/mL)
S1	16.57	33.14	0.00
S2	3.29	38.86	7.71
S3	13.29	11.14	10.00
S4	0.00	22.29	3.29
S5	20.00	0.00	6.71
S6	26.71	27.71	8.86
S7	10.00	50.00	5.57
S8	30.00	16.57	4.43
S9	23.29	44.57	2.29
S10	6.71	5.71	1.14

Sample	BSA (mg/mL)	Sucrose (mg/mL)	Methionine (mg/mL)
V1	16.00	30.29	0.57
V2	4.00	35.14	7.57
V3	13.00	10.29	9.43
V4	1.00	20.29	3.57
V5	19.00	0.51	6.43
V6	25.00	25.14	8.57
V7	10.00	45.14	5.57
V8	28.00	15.43	4.57
V9	22.00	40.00	2.57
V10	7.00	5.43	1.57

Figure 2. Samples information for model transferability studies. The concentrations were calculated using the design of experiment (DoE) approach, calculated by the Uniform Design (UD) algorithm.

Training sample	BSA (mg/mL)	Sucrose (mg/mL)	Methionine (mg/mL)
S-ID 1 (Batch 1)	28.57	28.77	7.14
S-ID 2 (Batch 2)	28.77	28.57	7.07
S-ID 3 (Batch 3)	28.37	28.37	7.21
Mean	28.57	28.57	7.14
Std Dev	0.20	0.20	0.07

Validation sample	BSA (mg/mL)	Sucrose (mg/mL)	Methionine (mg/mL)	Description	Attributes	Expectation quality outcome
V-ID 1	28.57	28.57	0.00		Missing formulation	Fail
V-ID 2	28.57	0.00	7.14		Missing formulation	Fail
V-ID 3	14.29	28.57	7.14		Wrong formulation	Fail
V-ID 4	0.00	28.57	7.14		Missing formulation	Fail
V-ID 5	28.57	28.57	7.30		Wrong formulation	Fail
V-ID 6	28.57	42.86	0.00		Missing formulation	Fail
V-ID 7	28.57	28.57	7.14	Lysozyme added as contaminant mimic	Contamination	Fail
V-ID 8	28.57	19.87	7.14	Glucose 4.58 mg/mL and fructose 4.58 mg/mL added	Sucrose hydrolyzes to glucose and fructose in acidic environment during storage.	Fail
V-ID 9	28.57	0.00	7.14	Glucose 15.05 mg/mL and fructose 15.05 mg/mL added	Complete excipient degradation	Fail
V-ID 10	28.57	28.57	7.14	Trypsin added.	Simulation of protein degradation. Trypsin cleave BSA to peptide fragments	Fail
V-ID 11	28.57	28.57	7.14		Correct formulation	Pass

Figure 3. Samples' information for identification and quality assessment.

Training data were collected on one instrument at one site, while the validation data were collected on six instruments at another site. Samples were frozen and shipped between sites. The study therefore reflects typical variations in storage, transport, and method transfer across instruments, locations, and operators. To demonstrate transfer function based interinstrument model transferability, an additional BSA set from 0 to 20 mg/mL in tris buffer at pH 8.0 was prepared in 5 mL glass vials.

For identification and quality assessment, three training batches were prepared with slightly different concentrations to mimic batch to batch variability (Figure 3). Validation samples represented correct formulation, wrong or missing formulation, contamination, excipient degradation, and active pharmaceutical ingredient (API) degradation. All samples were prepared in tris buffer at pH 8.0 as 4 mL fills in 5 mL borosilicate glass vials.

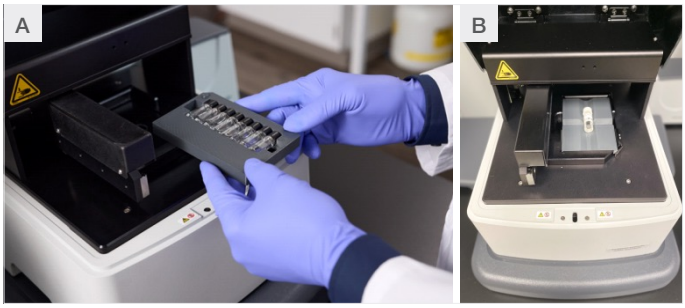

Figure 4. Eight and single vial sample holder accessories for DXR3 SmartRaman+ spectrometer are shown in A and B, respectively. Though not shown here, varieties of another sample holder are also available.

Raman data collection

Raman data were acquired using the DXR3 SmartRaman+ spectrometer with the sample holder, shown in Figure 4A. Acetaminophen showed minimal fluorescence, so a 532 nm laser was used. Acquisition parameters were as follows: 3 s integration time, 10 averages, 40 mW laser power, and a 50 µm aperture slit. Samples were positioned at X = 59,000 µm and Y = 39,000 µm. The Z-axis was adjusted manually to focus the laser inside the sample. The final Z coordinate was 3500 µm. The glass contributed minimal interference at 532 nm, so manual Z coordinate optimization was performed using the spectral region 500 to 1850 cm^{-1}.

BSA samples were tested with both 785 nm and 532 nm lasers using a single sample vial holder shown in Figure 4B. Due to high fluorescence background with 532 nm laser source, the 785 nm laser was selected for further BSA analysis. A key challenge with 785 nm is photoluminescence from borosilicate glass. This was mitigated by precise X, Y, and Z focusing of the DXR3 SmartRaman+ spectrometer to place the laser within the liquid, reducing glass signal and enhancing sample signal. The X and Y coordinates used in this study were set to the values obtained during the USP qualification test for the polystyrene in the built-in software . The Z-axis was optimized using principal component analysis (PCA) with 4 mL of 20 mg/mL BSA in tris buffer at pH 8.0 in 5 mL borosilicate vials. The optimized coordinates were used for all studies and across instruments. *Note, the Z-axis optimization performed in this study is not a part of the software.*

The signal to noise ratio (SNR) was optimized manually using different acquisition settings. Final acquisition settings were these : 150 mW laser power, 3 s integration time, 100 averages, 50 µm aperture slit, cosmic ray reduction set to “auto”, fluorescence correction none, and automatic dark background collect on. Single spectra were collected per sample, consistent with QC practice.

For transfer function based model transferability, a PLS model for BSA quantification was trained on the Thermo Scientific™ MarqMetrix™ All-In-One Raman Process Analyzer (MM AIO) using a 785 nm laser, 200 mW power, 3 s integration time, and 50 averages. Data was collected through glass vials using the Thermo Scientific™ MarqMetrix™ Proximal BallProbe™ Sampling Optic. An internal sample holder positioned the vial to focus within the sample and minimize glass signal. Validation samples were acquired on the DXR3 SmartRaman+ instrument with a 785 nm laser, 150 mW power, 3 s integration time, 80 averages, and a 50 µm slit aperture. Samples were positioned at X = 59,000 µm, Y = 39,000 µm, and Z = 3500 µm.

Chemometric model development

The Partial Least Squares (PLS) model for the acetaminophen quantification model was developed using the spectral region of 206 to 1875 cm^{-1} and 2731 to 3009 cm^{-1}. The Raman spectra were preprocessed using Savitzky-Golay filter (1st derivative, order = 2, window width = 13), followed by standard normal variate (SNV) normalization and mean centering. The optimum number of latent variables (LVs) was determined using leave-one-out cross-validation (LOOCV) and the trained model was evaluated using the variable importance in projection (VIP) score. The performance of the direct model transferability of the trained model was assessed by applying it to validation data acquired on five different instruments. The root mean square error of prediction (RMSEP), R^2 prediction, and prediction bias were statistics used to evaluate model performance.

For BSA, sucrose, and methionine quantification, PLS models used 323–3152 cm^{-1} with the same preprocessing (Savitzky-Golay 1st derivative, order = 2, window = 13; SNV; mean centering) and LV selection by LOOCV. Models were examined using VIP scores and selectivity ratio plots, and a PLS based limit of detection was calculated on a single instrument following the referenced guidance.[6] Performance was then assessed on validation data from six instruments using RMSEP, R^2 prediction, and prediction bias.

The transfer function based model centric calibration transfer (MCCT) was used to transfer a model from one instrument type to another. The primary instrument was the MM AIO, and the secondary (slave) instrument was the DXR3 SmartRaman+ spectrometer. A PLS model for BSA quantification was developed on MM AIO using training data preprocessed with a Savitzky-Golay filter (1st derivative, order = 2, window width = 13) and SNV normalization. DXR3 SmartRaman+ spectra were interpolated to the MM AIO Xaxis. The interpolated DXR3 SmartRaman+ data were then used for direct prediction with the MM AIO PLS model. Raman spectra from two additional samples (3 mg/mL and 13 mg/mL) were collected on both MM AIO and DXR3 SmartRaman+ instruments. After interpolation to a common X-axis, these paired spectra were used to compute a transfer function with pairwise direct standardization (PDS). The transfer function was inserted into the PLS workflow after the Savitzky-Golay filter step. The updated model was used to re-predict the test data from DXR3 SmartRaman+.

Finally, a principal component analysis (PCA) model was developed for identification and quality assessment. The spectral region from 400 to 3100 cm^{-1} was selected, followed by Savitzky-Golay filtering (1st derivative, order = 2, window width = 13) and SNV normalization. Scores less than 1 for reduced Hotelling T^2 and reduced Q residual were set as the threshold for “Pass,” while scores greater than 1 for Hotelling T^2 or reduced Q residual, or both, were set as the threshold for “Fail” with 95% confidence interval.

All chemometric work was performed using Solo Model Exporter 9.5 (2025) by Eigenvector Research, Inc., Manson, WA, USA.

Results and discussion

Direct model transferability: Acetaminophen samples through glass using a 532nm laser

A 532 nm laser was used to acquire Raman spectra from acetaminophen samples. Glass vials showed minimal photoluminescence at 532 nm, and acetaminophen had low fluorescence under this source. A PLS model for acetaminophen quantification was developed on a single primary instrument using the fingerprint and CH stretching region with two latent variables. The spectral region after Savitzky–Golay filtering and SNV normalization is shown in Figure 5A. Spectra are color coded by acetaminophen concentration (yellow = high, dark blue = low). The VIP score plot is shown in Figure 5B. Raman shifts with VIP > 1 were considered important.[7] Comparing Figures 5A and 5B shows that the important Raman shifts in the model aligned with acetaminophen signals, indicating model selectivity.

Model performance was validated using independent test data collected on five independent SmartRaman+ instruments. Test spectra were interpolated to the primary instrument's X axis, and the PLS model was applied directly. Predictions from the direct transfer are shown in Figure 5C. *The average RMSEP was 0.28 mg/mL, prediction bias was 0.19 mg/mL, and R^2 prediction was 0.99 (Figure 5C inset) for the concentration range of 0 to 10 mg/mL, demonstrating efficient direct transfer across DXR3 SmartRaman+ instruments.*

Error analysis by instrument showed that bias was the dominant contributor (Figure 5D; blue = RMSEP, orange = bias). Several strategies can correct bias, including applying a bias-correction factor, augmenting the data from multiple instruments to capture instrument specific variations, optimizing preprocessing to remove systematic spectral shifts, variable selection-based model optimization, hyper-tuning models' parameters, or adjusting the model's slope and intercept to realign predictions with reference values using transfer functions. A transfer function approach is discussed later. *Here, a simple bias correction markedly reduced error (green bar figure 5D), decreasing the average RMSEP from 0.28 mg/mL to less than 0.10 mg/mL.*

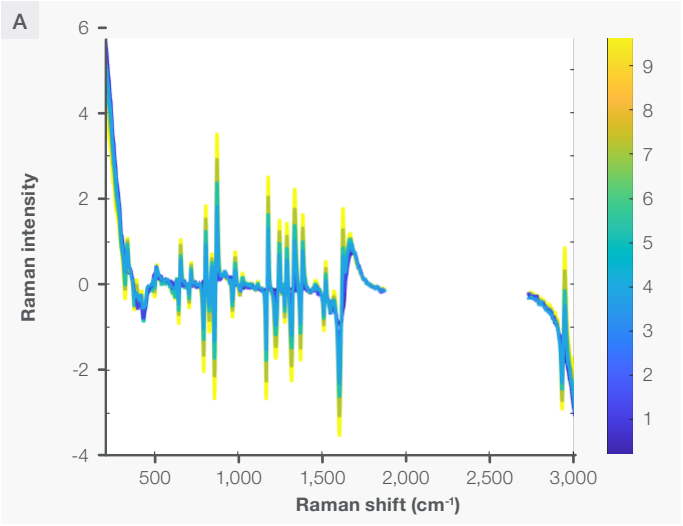

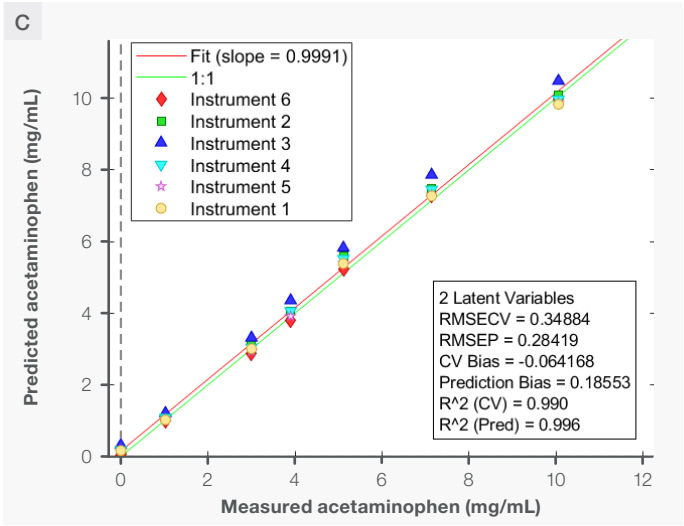

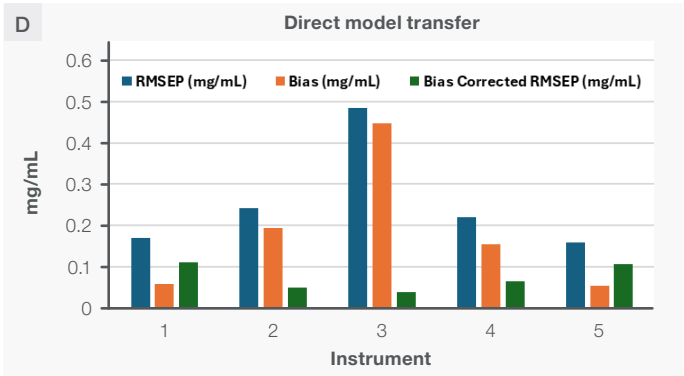

Figure 5. Direct model transferability across DXR3 SmartRaman+ using a 532 nm laser with through vial measurements. (A) Spectral region used for modeling after preprocessing; spectra are color coded by acetaminophen concentration. (B) VIP score plot; Raman shifts with VIP > 1 correspond to acetaminophen Raman signatures. (C) Correlation plot of predictions across five instruments; prediction statistics shown in the inset. Instrument 6 (training instrument) was not included to calculate prediction statistics (D) Instrument specific error analysis.

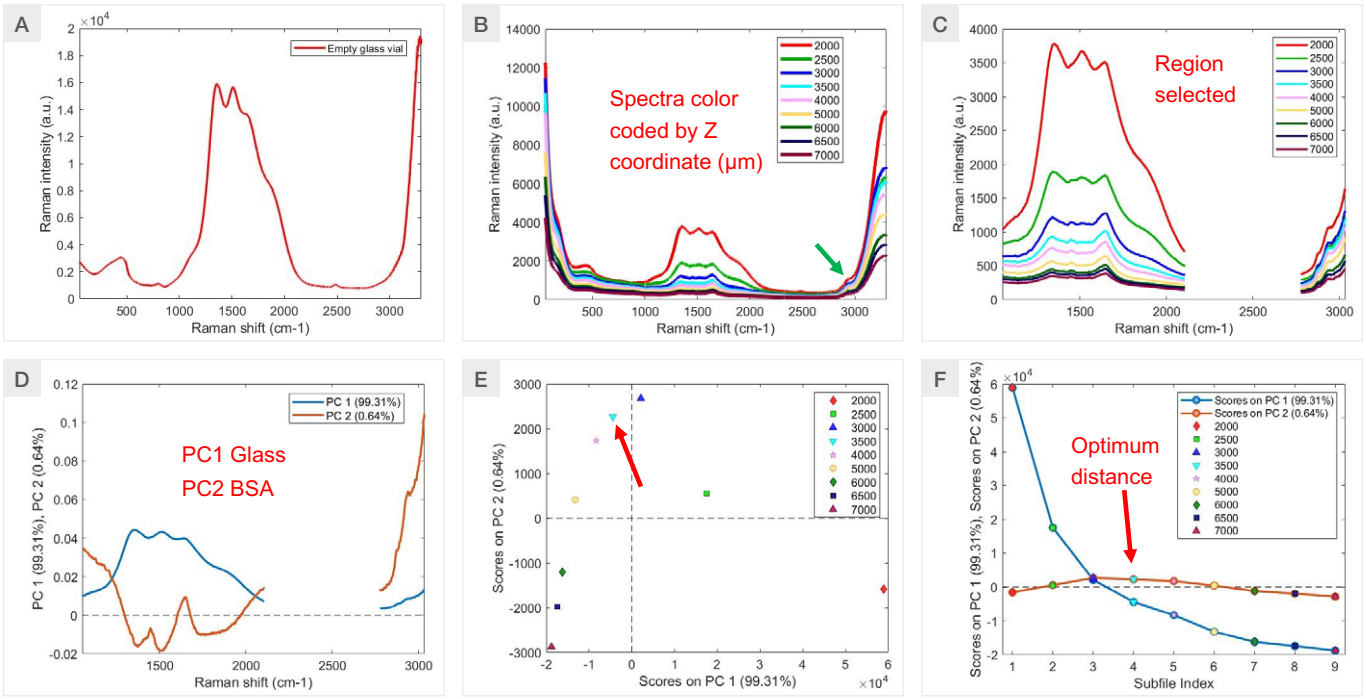

Figure 6. Workflow to minimize glass signal and enhance sample signal with a 785 nm laser: (A) empty glass spectra; (B) spectra at varying Z-axis positions; (C) regions selected for PCA; (D) loadings for PC1 and PC2; (E–F) scores on PC1 and PC2 identifying optimal value of Z = 3500 µm, shown by red arrows.

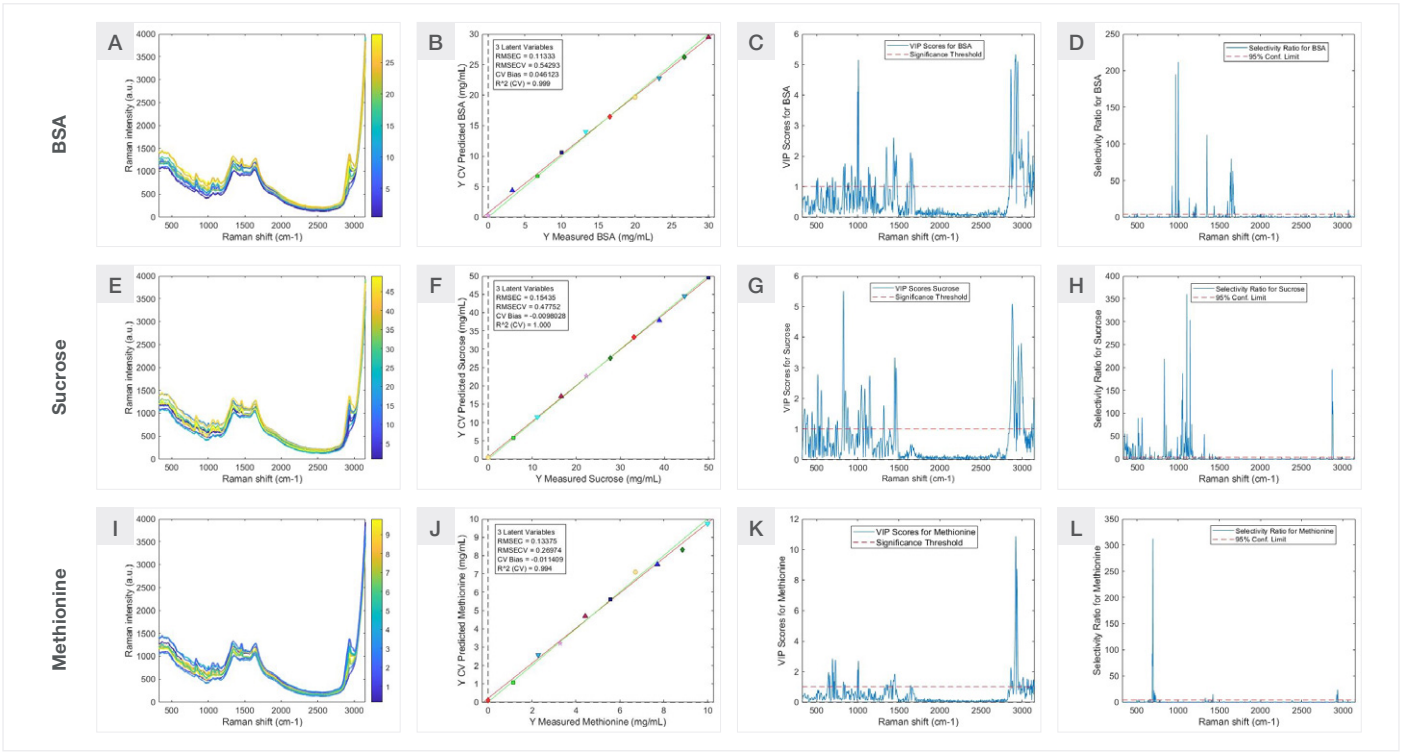

Figure 7. PLS calibration and specificity for BSA, sucrose, and methionine. (A, E, I) Through vial spectra are color coded by respective concentration. (B, F, J) Calibration plots with RMSECV (BSA = 0.54 mg/mL, sucrose = 0.48 mg/mL, methionine = 0.27 mg/mL) for the three latent variables PLS models used. (C, G, K) VIP scores highlighting key Raman bands (BSA: 1003, 1670 cm^{-1}; sucrose: 835 cm^{-1}; methionine: 700, 723 cm^{-1}). (D, H, L) Selectivity ratio plots also confirm analyte specific features.

Direct model transferability: Fluorescent BSA samples through glass using a 785 nm laser

Optimizing the sample position to minimize glass photoluminescence

Unlike the 532 nm laser, glass photoluminescence is a major interference when reading through a glass container with a 785 nm laser.[7] An overlay of spectra from an empty vial using 785 nm and 532 nm lasers is shown in SI 1 (see Supplementary Information section). Photoluminescence should be minimized to improve model performance and transferability across instruments as it's a variation associated with the container, not with analytes. While collecting the Raman spectra, the laser must pass through glass to reach the sample, so glass photoluminescence cannot be completely avoided. However, it can be reduced by adjusting the Z axis and focusing the laser into the sample. The workflow and results for Z axis optimization to reduce glass photoluminescence are shown in Figure 6.

Figure 6A shows Raman spectra of an empty glass container using a 785 nm laser. In addition to Raman bands at ~480 cm^{-1} (Si–O–Si bending), ~800 cm^{-1} (Si–O–Si symmetric stretching), and ~1080 cm^{-1} (Si–O–Si asymmetric stretching), the glass exhibits intense, broad photoluminescence spanning 1100–2200 cm^{-1}. [8] This photoluminescence may limit some through glass applications. Most biological samples in native or formulated states are highly fluorescent, making a 785 nm laser essential for many applications.

To address this, we acquired Raman spectra of 20 mg/mL BSA in a glass vial at different Z axis coordinates (2000–7000 µm) with fixed X = 59,000 µm and Y = 39,000 µm, as shown in Figure 6B. Unlike empty glass, BSA shows Raman features at ~2800–3100 cm^{-1} (CH stretching). Selecting 1100–2100 cm^{-1} and 2800–3100 cm^{-1} (Figure 6C), mean centering, and analyzing by PCA revealed that glass photoluminescence dominated principal component 1 (PC1), while the BSA amide I region (1640–1680 cm^{-1}) and CH stretching features were captured by PC2. Thus, the optimal Z axis setting is the one that minimized PC1 scores and maximized PC2 scores. As shown in Figures 6E and 6F, any Z-axis setting between 3000 to 6500 µm proved to be the optimal distance, as these spectra had similar features with minimal glass interferences. For this study, we selected the Z coordinate to be 3500 µm.

Quantitative BSA, sucrose, and methionine PLS model development

Calibration data for chemometric model development were acquired on a single primary instrument. The details of the PLS models for BSA, sucrose, and methionine, along with model statistics, are shown in Figure 7. The spectral regions used to develop the models for BSA, sucrose, and methionine are color coded by concentration in Figures 7A, 7E, and 7I. Three latent variables were selected for each PLS model. The root mean square error of cross validation (RMSECV) for BSA, sucrose, and methionine were 0.54 mg/mL, 0.48 mg/mL, and 0.27 mg/mL, respectively, for the tested concentration range (Figures 7B, 7F, and 7J).

The VIP and selectivity ratio plots were used to evaluate model specificity for the target analytes.[7] For BSA (Figures 7C and 7D), peaks at 1003 cm^{-1} and 1670 cm^{-1} are unique, corresponding to the phenylalanine ring breathing mode and the symmetric stretching of the carbonyl group in amide I.[9] For sucrose (Figures 7G and 7H), the 835 cm^{-1} band is specific and assigned to $\tau(CH_2)$ with contribution from ν(CC).[10] For methionine, the 700 and 723 cm^{-1} bands, assigned to C–S stretching,[11] dominate the VIP and selectivity plots. Comparing VIP and selectivity plots with aqueous spectra of BSA, sucrose, and methionine (Figure 8) shows that the dominant Raman shifts in the model are the characteristic Raman bands for each analyte, indicating high model specificity.

After developing the PLS models on the primary instrument and acquiring validation data on the same instrument, both datasets were combined to build augmented PLS models. Statistics from these augmented models were used to calculate the limit of detection (LOD) following the referenced guidance.[6] Results are summarized in Figure 9. *The LODs for BSA, sucrose, and methionine that could be confidently quantified in the tricomponent mixture under these specific experimental conditions were 0.80 mg/mL, 0.96 mg/mL, and 0.26 mg/mL, respectively.*

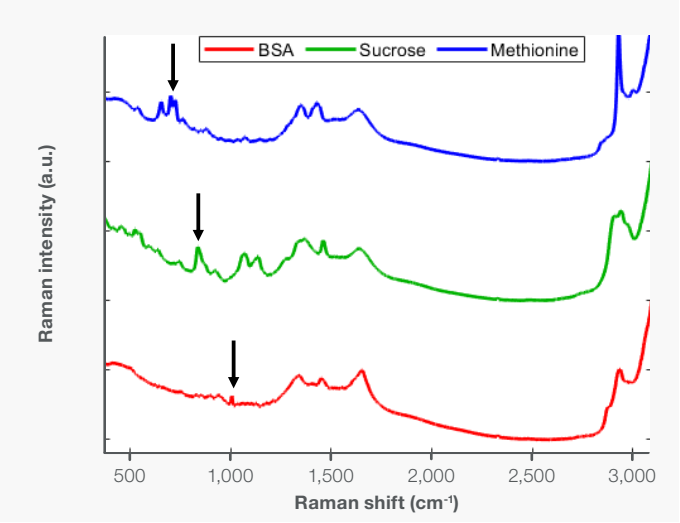

Figure 8. Characteristic Raman peaks for BSA, sucrose, and methionine, indicated by black arrows.

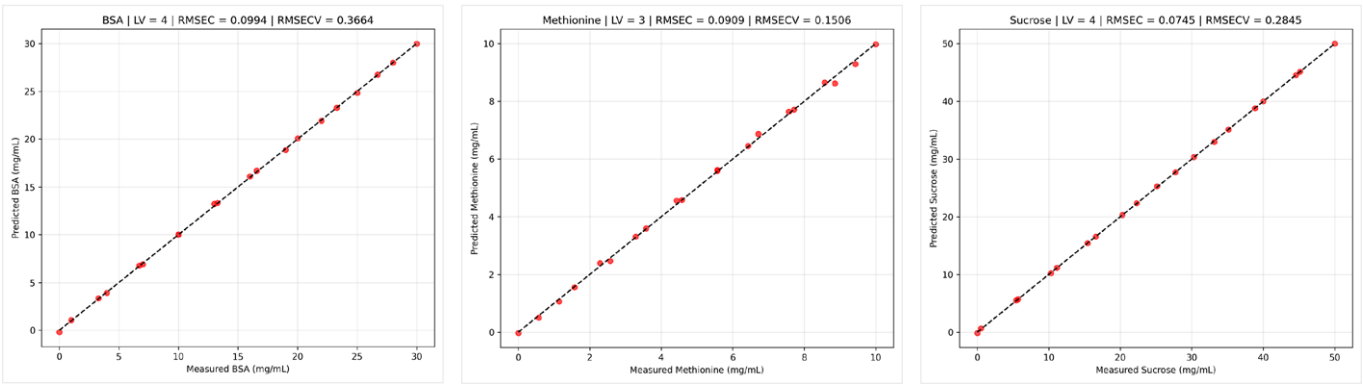

SUMMARY — ALL ANALYTES

Analyte	LV	RMSEC (mg/mL)	RMSECV (mg/mL)	LOD_min (mg/mL)	LOD_max(mg/mL)
BSA	4	0.0994	0.3664	0.7299	0.8043
Sucrose	4	0.0745	0.2845	0.8139	0.9649
Methionine	3	0.0909	0.1506	0.2431	0.2651

Figure 9. The LOD for BSA, sucrose, and methionine in the tricomponent mixture with under these experimental conditions were 0.80 mg/mL, 0.96 mg/mL, and 0.26 mg/mL respectively.

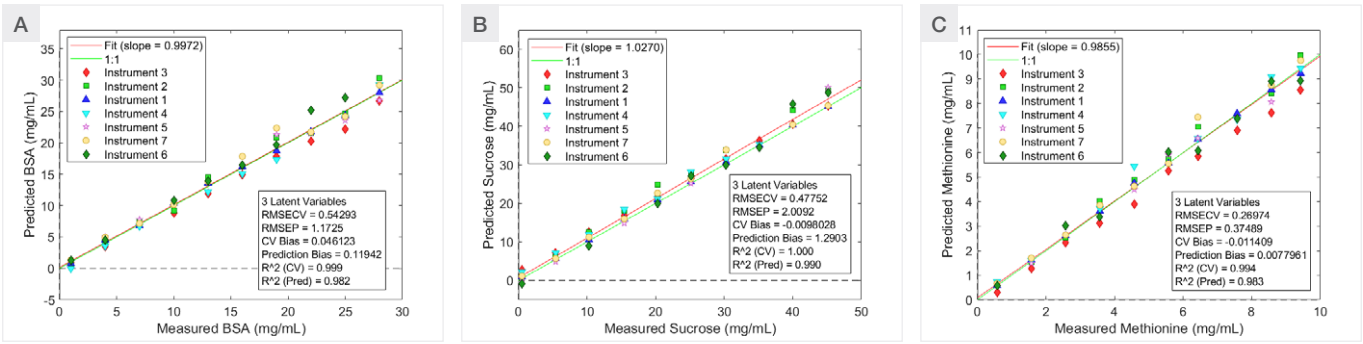

Figure 10. Direct model transferability across seven DXR3 SmartRaman+ instruments for BSA (A), sucrose (B), and methionine (C). The average RMSEP, prediction bias, and prediction R^2 were BSA, sucrose and methionine were 1.17 mg/mL, 0.12 mg/mL, 0.98, 2.00 mg/mL, 1.30 mg/mL, 0.99, 0.37 mg/mL, 0.01 mg/mL, and 0.98 respectively.

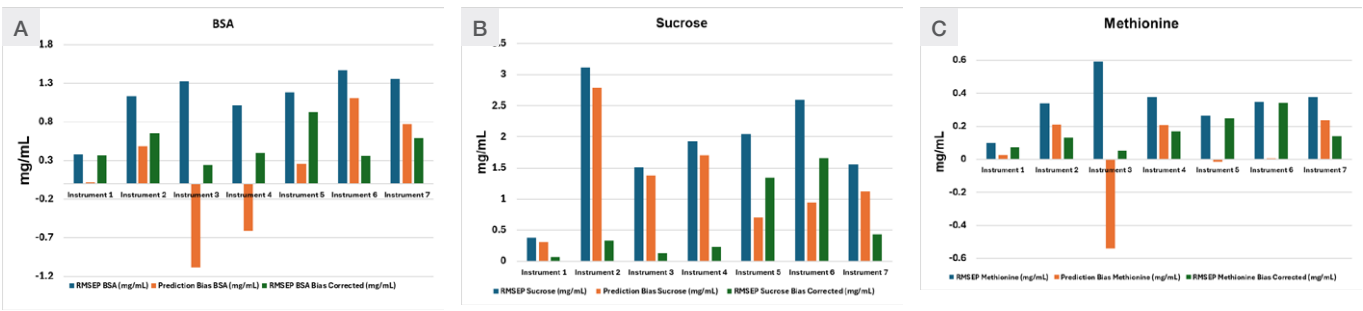

Figure 11. Error distribution across each instrument. The original RMSEP, bias and bias corrected RMSEP were represented by blue, orange, and green bars, respectively. The major error contribution is bias, which when removed significantly reduces prediction errors.

Direct model transferability for BSA, sucrose, and methionine quantification

To evaluate direct model transferability across DXR3 SmartRaman+ instruments, Raman spectra from validation samples were collected on six secondary instruments using the same acquisition settings as those used to develop the calibration model on the primary instrument, and the PLS models were applied directly to these spectra. The results are shown in Figure 10A (BSA), 10B (sucrose) and 10C (methionine). *The average RMSEP across seven instruments was 1.17 mg/mL for BSA, 2.00 mg/mL for sucrose, and 0.38 mg/mL for methionine within the respective concentration ranges of 0-30 mg/mL, 0-50 mg/mL, and 0-10 mg/mL, with all prediction errors remaining below 5% of the training concentration range.* Prediction biases for BSA, sucrose, and methionine were 0.12, 1.30, and 0.01 mg/mL, and the R^2 values for all analytes exceeded 0.98 as shown in inset in correlation plots, demonstrating effective direct model transferability when reading through glass vials using a 785 nm laser source.

Instrument-specific RMSEP (blue bars) and bias (orange bars), as shown in Figure 11A (BSA), 11B (sucrose), and 11C (methionine), indicated that most prediction errors stemmed from systematic positive or negative bias, aligned with trends reported in the literature for multivariate model transfer across spectroscopic instruments. Applying a simple bias correction substantially reduced the average RMSEP by more than 50% of the original RMSEP for BSA, sucrose, and methionine to 0.50, 0.59, and 0.17 mg/mL, respectively, as shown by green bars in Figure 11.

In this study, three primary sources of error were identified as the photoluminescence variability of the glass vials, subtle optical and mechanical differences between instruments, and variations introduced by sample preparation, freezing, shipping, and multi-site handling. Even with these sources of variability, the average original RMSEP values below 5% of the concentration range confirm strong model transferability across DXR3 SmartRaman+ instruments. This reflects the uniformity of their mechanical and optical design. These results provide a baseline expectation for users and indicate that, depending on application-specific tolerance limits, prediction performance may be further improved by expanding training data to capture glass photoluminescence variability, incorporating data from multiple instruments, or applying transfer learning approaches. As a proof-of-concept, a transfer learning approach is discussed below.

Transfer function assisted inter-instrument model transferability: A case study for bias correction

To illustrate model transferability using a transfer-function approach, a proof-of-concept experiment was conducted to transfer a BSA quantification model from one instrument type to another that is significantly different in mechanical and optical configurations (see Figure 12). A PLS model for BSA was first developed using spectra collected through glass vials with a 785 nm laser on the Thermo Scientific MarqMetrix All-in-One (MM AIO) process Raman analyzer. A one-latent-variable PLS model was selected as optimal, providing an RMSECV of 0.67 mg/mL over the training concentration range of 0 to 20 mg/mL (Figure 12B), and the associated VIP scores (Figure 12C) indicated that the model was dominated by the phenylalanine breathing mode near 1003 cm^{-1}. Validation data were then acquired on DXR3 SmartRaman+ spectrometer. Unlike the MM AIO, the DXR3 SmartRaman+ instrument implements a relative Y-axis correction using white-light calibration, resulting in substantial differences in the spectral response between the two instruments (Figures 12A and 12D. After interpolating the DXR3 SmartRaman+ spectra to the X-axis of the MM AIO, direct application of the MM AIO model yielded large prediction errors, with an RMSEP of 5.40 mg/mL and a prediction bias of 5.27 mg/mL (Figure 12E), along with elevated reduced Q residuals (Figure 12F), demonstrating poor direct model transferability.

To address this, a model-centric calibration transfer (MCCT) was performed using the PDS algorithm in SOLO Eigenvector software. Two samples were measured on both instruments, and the resulting spectra were used to generate a transfer function inserted into the model after the Savitzky-Golay preprocessing step. Incorporation of this transfer function markedly improved prediction performance, reducing the RMSEP and prediction bias to 0.87 mg/mL and 0.56 mg/mL, respectively (Figure 13A), and lowering the reduced Q residuals from approximately 20-25 to less than 1.5 (Figure 13B). These results demonstrate excellent inter-instrument model transferability from MM AIO to DXR3 SmartRaman+ instruments and show that transfer-function approaches can substantially reduce prediction errors dominated by bias. Although effective, this approach requires developing model- and instrument-specific transfer functions, which may be challenging in applications involving multiple models or multiple instruments.[12,13]

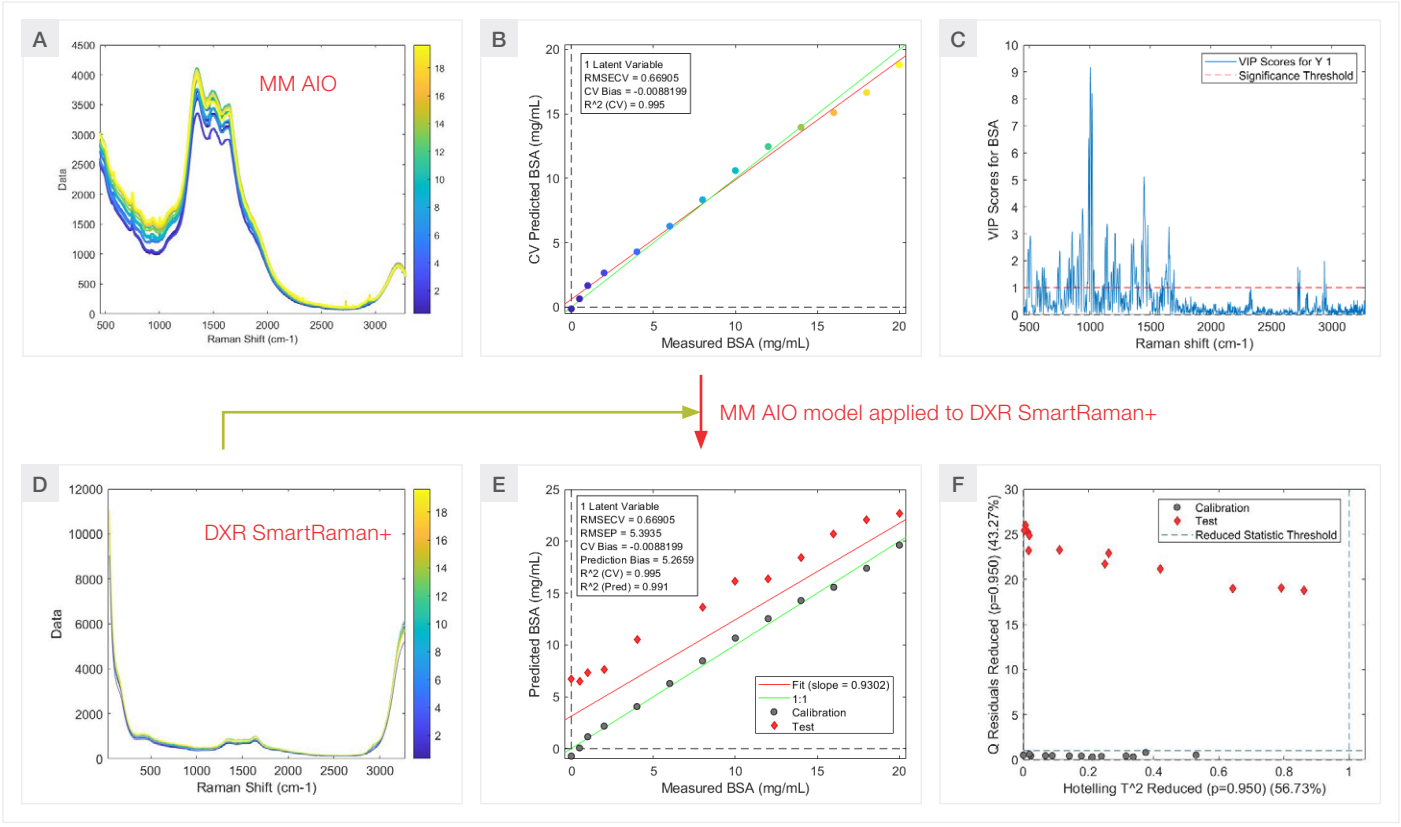

Figure 12. Spectral differences between the MM AIO (A; calibration) and DXR3 SmartRaman+ (D; test) instruments and their impact on direct model transferability are shown. The BSA PLS model developed on MM AIO (B, C) performed poorly when directly applied to DXR3 SmartRaman+ data, resulting in high prediction error and bias (E; grey (calibration) and red (test)) and elevated reduced Q-residuals (F; grey (calibration) and red (test)), indicating inadequate direct transferability between the two instrument platforms.

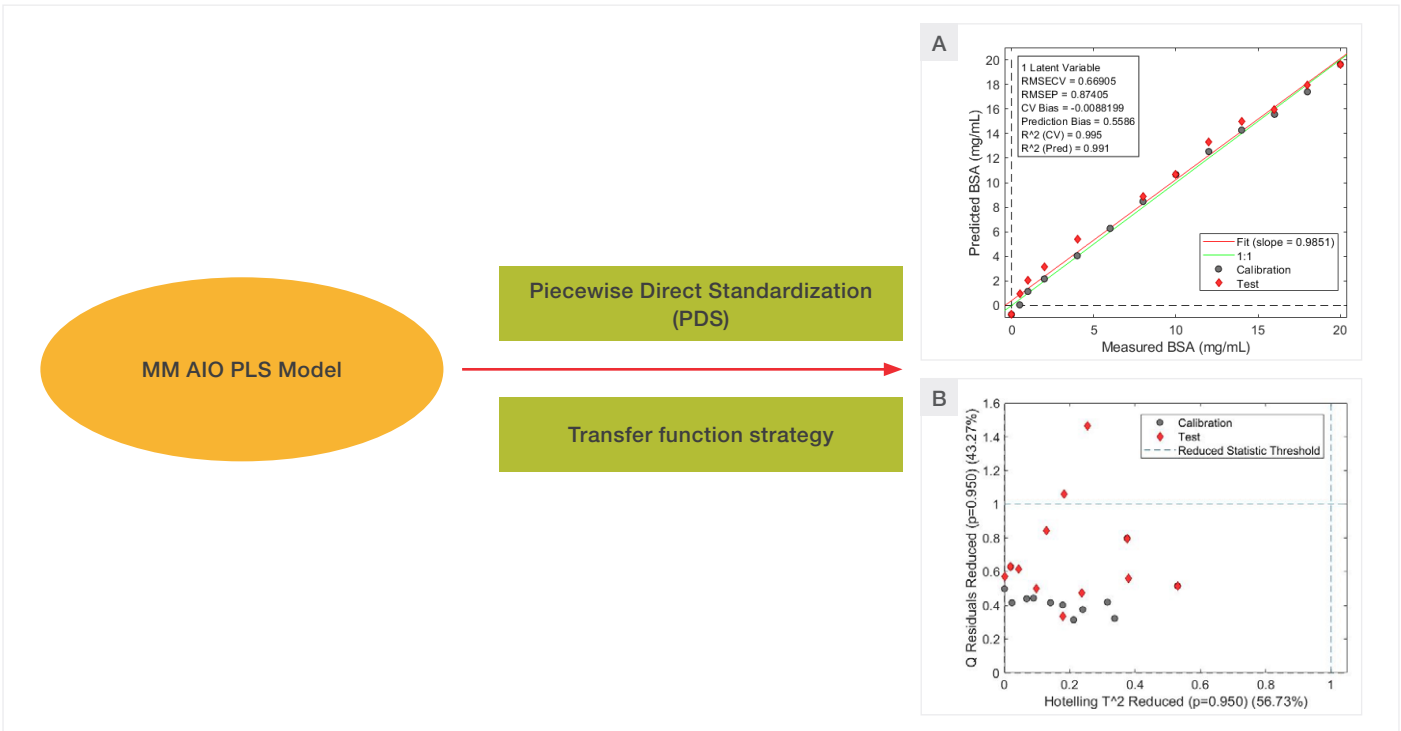

Figure 13. Inter-instrument model transfer using a piecewise direct standardization (PDS) transfer function. Incorporating the PDS transfer function into the MM AIO PLS model markedly improved prediction accuracy on DXR3 SmartRaman+ data, lowering both RMSEP and bias (A; grey (calibration) and red (test)) and lowering reduced Q residuals to acceptable levels (B; grey (calibration) and red (test)) of approximately close to 1.

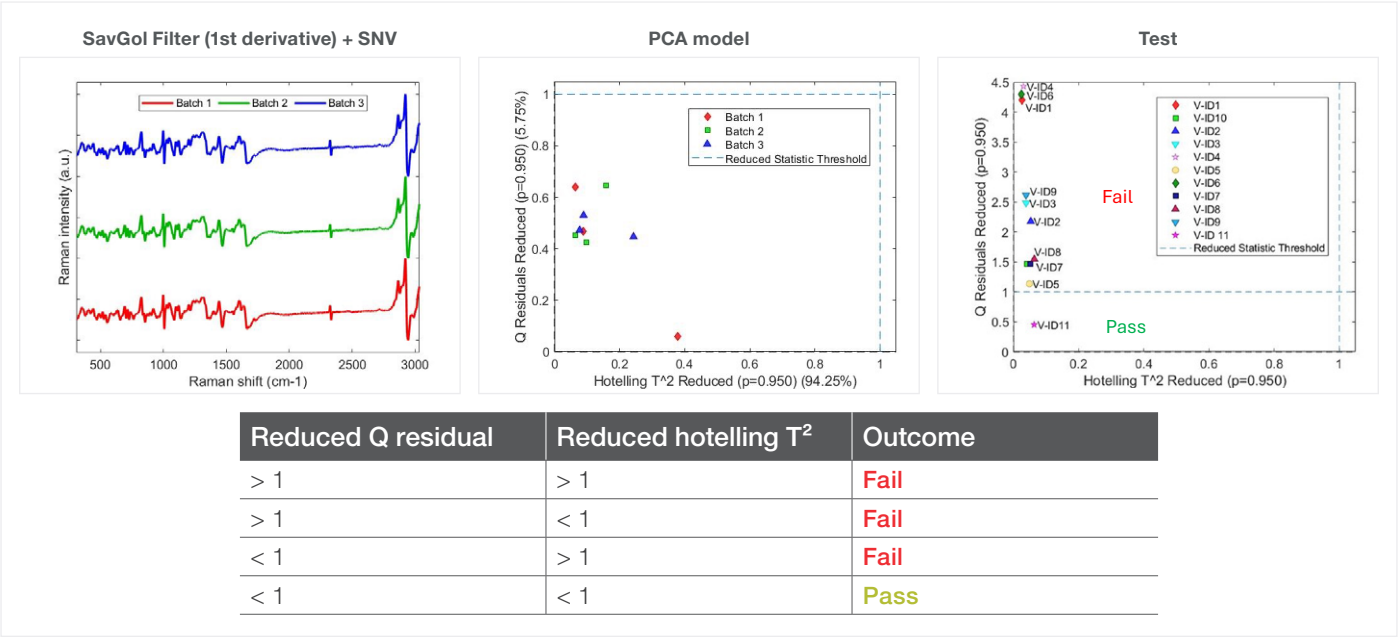

Reduced Q residual	Reduced hotelling T^2	Outcome
> 1	> 1	Fail
> 1	< 1	Fail
< 1	> 1	Fail
< 1	< 1	Pass

Figure 14. PCA model development and model results on validation data.

Validation sample	BSA (mg/mL)	Sucrose (mg/mL)	Methionine (mg/mL)	Description	Attributes	Expectation quality check	Model prediction
V-ID 1	28.57	28.57	0.00		Missing formulation	Fail	Fail
V-ID 2	28.57	0.00	7.14		Missing formulation	Fail	Fail
V-ID 3	14.29	28.57	7.14		Wrong formulation	Fail	Fail
V-ID 4	0.00	28.57	7.14		Missing formulation	Fail	Fail
V-ID 5	28.57	28.57	7.30		Wrong formulation	Fail	Fail
V-ID 6	28.57	42.86	0.00		Missing formulation	Fail	Fail
V-ID 7	28.57	28.57	7.14	Lysozyme added as contaminat mimic	Contamination	Fail	Fail
V-ID 8	28.57	19.87	7.14	Glucose 4.58 mg/mL and fructose 4.58 mg/mL added	Sucrose hydrolyzes to glucose and fructose in acidic environment during storage.	Fail	Fail
V-ID 9	28.57	0.00	7.14	Glucose 15.05 mg/mL and fructose 15.05 mg/mL added	Complete excipient degradation	Fail	Fail
V-ID 10	28.57	28.57	7.14	Trypsin added.	Simulation of protein degradation. Trypsin cleave BSA to peptide fragments	Fail	Fail
V-ID 11	28.57	28.57	7.14		Correct formulation	Pass	Pass

Figure 15. Test sample description and results from model predictions.

Identification and quality assessment of fill-finish drug products

The capability of DXR3 SmartRaman+ spectrometer for fill-finish identification and quality assessments is illustrated in Figure 14. The PCA component model was developed using three principal components after applying Savitzky-Golay filtering (1st derivative, order = 2, window width = 13) and SNV normalization. The training samples from Batches 1, 2, and 3 were confined within the model space spanned by the reduced Q residual = 1 and reduced Hotelling T^2 = 1 with 95% confidence interval. Hence, the "Pass" or "Positive Identification" criteria were set only for samples that have reduced Q residual < 1 and reduced Hotelling T^2 < 1. Users may set other values of reduced Q residual and reduced Hotelling T^2 at different confidence levels depending on their applications. The test data with different formulations were collected on the same instruments. The model was then applied to the test data. The reduced Q residual and reduced Hotelling T^2 scores were calculated for each validation sample after projecting the data into the PCA model space. The scores were used to assign "Pass" or "Fail" outcomes as shown in Figure 14 and Figure 15.

Validation samples V-ID 1–6, which were missing or incorrectly formulated relative to the training batches, exhibited reduced Q residuals > 1 and were flagged as "Fail." Sample V-ID 7 contained lysozyme as contaminant, and the additional Raman features introduced by this impurity also produced reduced Q residuals > 1, yielding a "Fail" outcome. Samples V-ID 8 and 9 modeled excipient degradation via sucrose hydrolysis to glucose and fructose, which altered their Raman signatures and resulted in reduced Q residuals > 1, consistent with a "Fail" classification. Sucrose has been shown to spontaneously undergo hydrolysis into glucose and fructose, most commonly due to acid-catalyzed hydrolysis. Previously, we have reported how Raman can be used to monitor sucrose concentration in the ultrafiltration/diafiltration (UF/DF) in real time as well as sucrose hydrolysis as a QC check during buffer storage.[14]

Sample V-ID 10 simulated the scenario of drug product degradation. A small amount of trypsin was added to the sample, which hydrolyzed BSA into peptides and amino acids. Hydrolysis of BSA triggered several distinct changes in the Raman spectra, including the loss of the amide I Raman signal. This is consistent with the mode of action of trypsin, which hydrolyzes amide I bonds. Therefore, the sample had reduced Q residual > 1, resulting in "Fail" identification.

Finally, sample V-ID 11 matched the formulation of the training batches, produced reduced Q residual < 1, and therefore passed the identification criteria.

Conclusions

- Robust direct model transferability across DXR3 SmartRaman+ instruments was demonstrated using both 532 nm and 785 nm excitation for through-glass measurements. Prediction errors (RMSEP) remained below 5% of the tested concentration ranges, confirming reliable quantitative performance across multiple instruments.
- Residual prediction errors were dominated by systematic bias, primarily arising from glass photoluminescence, subtle optical and mechanical differences between instruments, and sample handling effects such as freeze–thaw and transport.
- Instrument-specific error analysis showed that bias correction is highly effective, with simple bias removal reducing RMSEP by more than 50% for BSA, sucrose, and methionine. Additional performance gains may be achieved by incorporating multi-instrument data, optimizing preprocessing and variable selection, or applying model slope and intercept adjustments.
- A proof-of-concept transfer-function strategy successfully enabled inter-instrument model transfer between MM AIO and DXR3 SmartRaman+ platforms, substantially reducing prediction bias and error. This demonstrates a viable approach for extending calibration models across different Raman instrument architectures.
- The DXR3 SmartRaman+ spectrometer demonstrated strong capability for fill-finish drug product identification and quality assessment, reliably detecting formulation errors, contamination, and degradation using PCA-based classification.
- Overall, these results establish DXR3 SmartRaman+ as a versatile and automation-ready Raman platform for biopharmaceutical quality control, offering robust model portability, reliable multi-attribute measurements, and strong alignment with modern manufacturing and regulatory expectations.

References

1. Kesik-Brodacka, M. Progress in Biopharmaceutical Development. Biotechnol. Appl. Biochem. 2018, 65 (3), 306–322. https://doi.org/10.1002/bab.1617.
2. Wei, B.; Woon, N.; Dai, L.; Fish, R.; Tai, M.; Handagama, W.; Yin, A.; Sun, J.; Maier, A.; McDaniel, D.; Kadaub, E.; Yang, J.; Saggu, M.; Woys, A.; Pester, O.; Lambert, D.; Pell, A.; Hao, Z.; Magill, G.; Yim, J.; Chan, J.; Yang, L.; Macchi, F.; Bell, C.; Deperalta, G.; Chen, Y. Multi-Attribute Raman Spectroscopy (MARS) for Monitoring Product Quality Attributes in Formulated Monoclonal Antibody Therapeutics. mAbs 2022, 14 (1), 2007564. https://doi.org/10.1080/19420862.2021.2007564.
3. Ghosh, I.; Gutka, H.; Krause, M. E.; Clemens, R.; Kashi, R. S. A Systematic Review of Commercial High Concentration Antibody Drug Products Approved in the US: Formulation Composition, Dosage Form Design and Primary Packaging Considerations. mAbs 2023, 15 (1), 2205540. https://doi.org/10.1080/19420862.2023.2205540.
4. Rao, V. A.; Kim, J. J.; Patel, D. S.; Rains, K.; Estoll, C. R. A Comprehensive Scientific Survey of Excipients Used in Currently Marketed, Therapeutic Biological Drug Products. Pharm. Res. 2020, 37 (10), 200. https://doi.org/10.1007/s11095-020-02919-4.
5. Zhang, L.; Liang, Y.-Z.; Jiang, J.-H.; Yu, R.-Q.; Fang, K.-T. Uniform Design Applied to Nonlinear Multivariate Calibration by ANN. Anal. Chim. Acta 1998, 370 (1), 65–77. https://doi.org/10.1016/S0003-2670(98)00256-6.
6. Allegrini, F.; Olivieri, A. C. IUPAC-Consistent Approach to the Limit of Detection in Partial Least-Squares Calibration. Anal. Chem. 2014, 86 (15), 7858–7866. https://doi.org/10.1021/ac501786u.
7. Farrés, M.; Platikanov, S.; Tsakovski, S.; Tauler, R. Comparison of the Variable Importance in Projection (VIP) and of the Selectivity Ratio (SR) Methods for Variable Selection and Interpretation. https://doi.org/10.1002/cem.2736.
8. Liu, H.; Kaya, H.; Lin, Y.-T.; Ogrinc, A.; Kim, S. H. Vibrational Spectroscopy Analysis of Silica and Silicate Glass Networks. J. Am. Ceram. Soc. 2022, 105 (4), 2355–2384. https://doi.org/10.1111/jace.18206.
9. Peters, J.; Park, E.; Kalyanaraman, R.; Luczak, A.; Ganesh, V. Protein Secondary Structure Determination Using Drop Coat Deposition Confocal Raman Spectroscopy. 2016, 31, 31–39.
10. Wiercigroch, E.; Szafraniec, E.; Czamara, K.; Pacia, M. Z.; Majzner, K.; Kochan, K.; Kaczor, A.; Baranska, M.; Malek, K. Raman and Infrared Spectroscopy of Carbohydrates: A Review. Spectrochim. Acta. A. Mol. Biomol. Spectrosc. 2017, 185, 317–335. https://doi.org/10.1016/j.saa.2017.05.045.
11. Zhu, G.; Zhu, X.; Fan, Q.; Wan, X. Raman Spectra of Amino Acids and Their Aqueous Solutions. Spectrochim. Acta. A. Mol. Biomol. Spectrosc. 2011, 78 (3), 1187–1195. https://doi.org/10.1016/j.saa.2010.12.079.
12. Lang, Z.; Chen, G.; Yan, S.; Zhang, Z.; Yang, Y.; Tang, Z.; Zhu, H.; Dong, S.; Zhou, H.; Zhou, W. Enhancing Cross-Scale Raman in-Line Monitoring Capability of Cell Culture Process in Large-Scale Manufacturing. AIChE J. 2025, 71 (1), e18608. https://doi.org/10.1002/aic.18608.
13. Myers, N. M.; Gao, B.; Amchin, D.; Masucci, E. M.; Balss, K. M. Calibration Transfer Across Instrument Vendors for Bioprocess Raman Monitoring. AAPS J. 2025, 28 (1), 5. https://doi.org/10.1208/s12248-025-01156-0.
14. Nolasco, M.; Siemers, A.; Pleitt, K.; Khadka, N. Process Raman as a Comprehensive Solution for Downstream Buffer Workflow.

Supplementary information

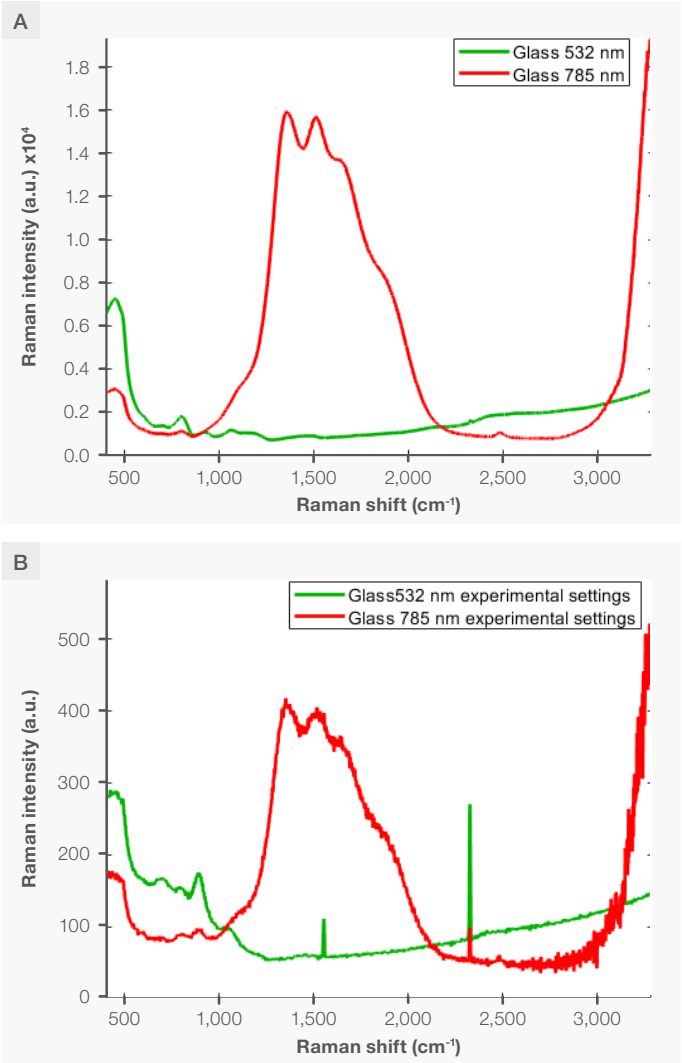

SI 1. Raman spectra of an empty glass vial collected using 785 nm (red) and 532 nm (green) excitation while focusing the laser directly on the glass surface (A). Under 785 nm excitation, strong glass photoluminescence obscures the 1000–2000 cm^{-1} spectral region. When the same acquisition parameters used in the main experiments were applied, the glass photoluminescence was significantly reduced (B), decreasing maximum intensity from approximately 15,000 counts to about 400 counts at ~ 1400 cm^{-1}.